Histol Histopathol (2019) 34: 513-523

http://www.hh.um.es

Histology and Histopathology

From Cell Biology to Tissue Engineering

Umbilical cord-derived mesenchymal stromal/stem cells enhance recovery of surgically induced skeletal muscle ischemia in a rat model

Irina Arutyunyan[1,2], Timur Fatkhudinov[1,2], Andrey Elchaninov[1,2], Olesya Vasyukova[3], Andrey Makarov[1,4], Natalia Usman[1], Evgeniya Kananykhina[1,3], Anastasiya Lokhonina[1,3], Dmitry Goldshtein[5], Galina Bolshakova[3] and Gennady Sukhikh[1]

[1]National Medical Research Center for Obstetrics, Gynecology and Perinatology named after Academician V.I. Kulakov of Ministry of Healthcare of Russian Federation, [2]Peoples' Friendship University of Russia (RUDN University), [3]Scientific Research Institute of Human Morphology, [4]Pirogov Russian National Research Medical University, Ministry of Healthcare of the Russian Federation and [5]Research Centre of Medical Genetics of the Russian Academy of Medical Sciences, Moscow, Russian Federation

Summary. This study delves into possible mechanisms underlying the stimulating influence of UC-MSCs transplantation on functional and structural recovery of ischemic skeletal muscles. Limb ischemia was created in Sprague-Dawley rats by excision of femoral and popliteal arteries. Allogeneic rat PKH26-labeled UC-MSCs were administered by direct intramuscular injection. Animals of experimental group responded to the transplantation by improvement in their locomotor function as assessed by the rotarod performance test on day 9 and 29 after transplantation. Histomorphometric analysis showed that relative area of the lesions in the experimental group was significantly smaller than in the control group at all time points during the observation. Calculated densities of microcirculation vessels within the lesions were significantly higher in the experimental group than in the control group on day 10 after transplantation. Only a part of the transplanted allogeneic UC-MSCs survived within the ischemic muscle tissue, and a considerable portion of these surviving cells were found alongside the VEGF-producing preserved muscle fibers. The PKH26 label was not found within the walls of capillaries or larger blood vessels. The administration of allogeneic UC-MSCs significantly increased the proportion of M2 macrophages, exhibiting proangiogenic and anti-inflammatory properties, for at least 10 days following the transplantation.

Key words: Umbilical cord-derived mesenchymal stromal/stem cells, Allogeneic transplantation, Muscle ischemia, Revascularization, M2 macrophage activation

Introduction

An estimated 10% of the population of western countries suffers from peripheral artery diseases most commonly resulting in lower limb ischemia. Despite outstanding achievements in the field of endovascular surgery, the problem is far from being solved. At the stage of critical limb ischemia, every third patient is subject to amputation surgery and 20% of the patients

Offprint requests to: Dr. T. Fatkhudinov, Laboratory of Regenerative Medicine, National Medical Research Center for Obstetrics, Gynecology and Perinatology named after Academician V.I. Kulakov of Ministry of Healthcare of Russian Federation, 4 Oparin Street, Moscow, 117997, Russian Federation. e-mail: tfat@yandex.ru

DOI: 10.14670/HH-18-057

Abbreviations: CD, cluster of differentiation; cluster designation; DAPI, 4',6-diamidino-2-phenylindole; FDA, Food and Drug Administration; FGFb, Basic fibroblast growth factor; FITC, Fluorescein isothiocyanate; HGF, Hepatocyte growth factor; HIF-1, Hypoxia-inducible factor 1; IGF-1, Insulin-like growth factor 1; IL-1β, Interleukin 1β; MCP-1, Monocyte chemoattractant protein-1; MMP9, Matrix metallopeptidase 9; MSCs, Mesenchymal stromal/stem cells; PDGF, Platelet-derived growth factor; PGF, Placental growth factor; SD, standard deviation; αSMA, α Smooth muscle actin; TNFα, tumor necrosis factor α; UC-MSCs, Umbilical cord-derived mesenchymal stromal/stem cells; VEGF, Vascular endothelial growth factor.

die within the first 6 months after diagnosis (Norgren et al., 2007).

Rapid development of cell technologies facilitated their introduction to the treatment of lower limb ischemia. According to the FDA clinical trials database, more than a hundred clinical trials of various cell types including smooth muscle cells, endothelial cells, subpopulations of CD133+ or CD34+ cells, mononuclear cells obtained from peripheral blood or bone marrow, and also mesenchymal stromal/stem cells (MSCs) isolated from bone marrow, adipose tissue, umbilical cord blood, or placenta are currently in progress.

Sources of particular stromal/stem cell varieties used for transplantation may influence the rates of revascularization and recovery. Some studies show no significant differences in therapeutic potential between stromal/stem cells obtained from different sources (for example, between allogeneic MSCs isolated from bone marrow and from fetal membranes (Ishikane et al., 2008)). The others demonstrate that therapeutic efficacy of cells, as manifested both *in vitro* and *in vivo*, may depend on their source of origin. For instance, the bone marrow-derived MSCs are shown to be less beneficial to recovery of blood flow in a mouse model of limb ischemia than the adipose tissue-derived MSCs (Kim et al., 2007), but more beneficial than the bone marrow-derived mononuclear cells (Iwase et al., 2005). Several strands of evidence support the concept of enhanced regenerative potential of MSCs isolated from perinatal tissues, as compared with MSCs isolated from adult tissues. In particular, the umbilical cord-derived mesenchymal stromal/stem cells (UC-MSCs), representing the perinatal MSCs, have enormous proliferative potential and show high rates of response to inductive stimuli that promote endothelial differentiation; they also have remarkable immuno-modulatory properties and are more resistant to hypoxic conditions than the adult cells, and can therefore be regarded as a favorable candidate for cell therapies (Kalaszczynska and Ferdyn, 2015; Arutyunyan et al., 2016a).

A characteristic feature of the UC-MSC phenotype is represented by shifted amounts of pro-angiogenic and anti-angiogenic factors in their secretome. Importantly, negligible amounts of the major proangiogenic factor VEGF-A (Vascular endothelial growth factor A) secreted by UC-MSCs *in vitro* (Arutyunyan et al., 2016a,b) call into question the whole issue of their efficacy in orchestrating tissue recovery from ischemic damage. Regardless of that, several studies have confirmed appropriateness of UC-MSC transplantation for the treatment of ischemic damage, as it significantly increases blood flow and stimulates angiogenesis in the ischemic skeletal muscle tissue (Zhang et al., 2012; Choi et al., 2013; Han et al., 2016). Moreover, preclinical studies have been undertaken to determine the optimal delivery method, the optimal timing of the transplantation (Liew and O'Brien, 2012), and the optimal number of cells in the transplant (Kang et al., 2016) for this particular model. At the same time, mechanisms underlying therapeutic action UC-MSCs remain understudied; these may include the substitution/transdifferentiation effect, and also the trophic and paracrine influences of the transplant on pro-inflammatory infiltrating cells, endothelial cells, and resident connective tissue cells in the damaged area (Dayan et al., 2011; Santos et al., 2013; Santos Nascimento et al., 2014; Sabapathy et al., 2014; Liu et al., 2014; Donders et al., 2015; Lin et al., 2015).

In our previously reported experiments we have shown that the UC-MSCs may be capable of participating in both the replacement and the paracrine mechanisms of stimulating tissue regeneration (because they are capable of differentiation into the endothelial cell-like CD31+ phenotype, and they also effectively stimulate proliferation, motility, and directed migration of endothelial cells *in vitro*) (Arutyunyan et al., 2016b). This study delves into possible mechanisms underlying the stimulating influence of UC-MSCs transplantation on functional and structural recovery of ischemic skeletal muscles *in vivo*.

Materials and methods

Cell cultures and labeling

The cells were obtained from intervascular tissue of rat umbilical cords by explant culture. Their identity as MSCs was proved by typical morphology, adhesive properties, robust clonogenic growth on the untreated plastic, specific cell surface antigen expression profiles, and differentiation capacities as previously described (Arutyunyan et al., 2015).

At the 3rd passage, the cells were labeled with PKH26 Red Fluorescent Cell Linker Kit (Sigma-Aldrich, St. Louis, MO, USA), washed twice with saline (PanEco, Moscow, Russia), and transferred to culture dishes for evaluation of the labeling, or directly to injection syringes.

Animals

Outbred Sprague-Dawley rats, body weight 300-400 g, were obtained from the stock of Institute of Bioorganic Chemistry branch facilities in Pushchino, Moscow region, Russia. Experimental work involving animals was carried out according to the rules of laboratory practice (National Guidelines No. 267 by Ministry of Healthcare of the Russian Federation, June 1, 2003), and all efforts were made to minimize suffering. The study was approved by Ethical Review Board at the Institute for Human Morphology (Protocol No. 8b, November 10, 2012).

Unilateral hindlimb ischemia induction and MSC injection

The animals were operated under general anesthesia

with zoletil, 20 mg/kg (Virbac, Carros, France), and rometar, 5 mg/kg (Bioveta, Ivanovice na Hané, Czech Republic). Sustained calf muscle ischemia with aseptic inflammatory response was induced by excision of femoral and popliteal arteries. The animals were randomized into two groups: (1) UC-MSCs administration and (2) saline administration (control group). The MSCs were injected via 27G needle into calf muscles at ten different points (totally 5×10^6 cells in 1 ml of saline) on day 7 after surgery.

The animals were sacrificed in CO_2-chamber 3, 10, or 30 days after transplantation (8 animals per time point), and calf muscle complexes including musculus (m.) tibialis cranialis, m. tibialis caudalis, m. triceps surae, m. gastrocnemius, m. soleus, m. plantaris, m. peroneus longus, and m. peroneus brevis were collected.

All data were collected and analyzed by independent observers blinded to animal randomization.

Rotarod performance test

The animals were subject to the rotarod performance test a day before surgery, a day before transplantation, and a day before sacrifice. The rats were placed on accelerating rotating rod; time length for which a rat stayed on the rod before falling from it was recorded in seconds.

Histomorphometry

All chemicals used for histological tissue processing were obtained from BioVitrum, Saint-Petersburg, Russia. The tissues were fixed in 10% neutral phosphate buffered formalin for 72 hours, subsequently washed in running tap water for 24 hours, dehydrated, embedded in paraffin, and 5 μm thick transverse sections were cut from three levels using manual microtome. The sections were rehydrated, stained with hematoxylin and eosin, dehydrated, and mounted for observation.

Images at magnification of ×200 were taken with Leica DM 2500 microscope and ImageScope M software (Leica Microsystems, Heidelberg, Germany).

Volume density of damaged tissue (including necrotized and atrophied muscle fibers) was measured using the 25-point lattice calculation technique, by taking 750 points per individual (25 points per field of view multiplied by 10 randomly chosen fields of view multiplied by 3 levels of cutting).

Immunohistochemistry

The tissues were frozen in liquid nitrogen, and 5-6 μm thick cryosections from four levels were prepared. The sections were stained with anti-CD68 (macrophage-specific; ab125212, Abcam, Cambridge, MA, USA), anti-CD206 (M2 activated macrophage-specific; sc-34577, Santa Cruz Biotechnology, Santa Cruz, CA, USA), anti-VEGF (ab 9570, Abcam), anti-CD31 (endothelial cell-specific; ab 24590, Abcam), or anti-αSMA (smooth muscle cell actin-specific; ab5694, Abcam) antibody at a dilution of 1:200 followed by FITC-conjugated secondary antibody (ab97050 or ab6785, Abcam) according to the manufacturers' protocols; the nuclei were counterstained with DAPI (Sigma-Aldrich). Images at magnification of ×400 were taken with Leica DM 4000 B fluorescent microscope and LAS AF v.3.1.0 build 8587 software (Leica Microsystems).

Microcirculation vessels were calculated using Adobe Photoshop CS6 software, for 30 randomly chosen fields of view per level of cutting.

Relative numbers of the CD68+ and CD206+ cells (i.e. relations of specifically stained cell numbers to the total cell number) were calculated for 100 fields of view per individual (25 fields of view multiplied by 4 levels of cutting).

Confocal microscopy

Colocalization analysis of confocal fluorescence images was performed on cryosections stained with anti-CD68 antibody (ab125212, Abcam). The images were taken with Carl Zeiss LSM700 confocal laser microscope and ZEN software (Carl Zeiss, Jena, Germany). The Manders' overlap coefficients were determined using 10 fields of view per individual.

Statistics

The data were analyzed using Sigma Stat 3.5 software (Systat Software Inc., San Jose, CA, USA) and expressed as mean±standard deviation (SD). Student's t-test was used for pairwise comparisons between groups of normally distributed values, whereas the Mann-Whitney test was applied for distributions differing from normal; P values <0.05 were considered significant.

Results

Comparative in vivo assessment of functional response to ischemic damage

The surgical stress response was of moderate intensity, and the mortality constituted 0.0%. On days 1 and 2 the operated limb was totally immobile, on day 7 the rats moved actively around with some dragging of the affected hindlimbs, and no symptoms of gangrene were observed.

The surgery produced an immediate rotarod performance deterioration. In the control group, duration of rotarod performance further decreased from 20.8±0.7 s a day before transplantation to 8.0±2.4 s on day 29 after transplantation. In the experimental group, the decrease was less pronounced (from 21.0±0.6 s to 15.2±1.4 s, respectively). Accordingly, on days 9 and 29 after transplantation the duration of rotarod performance in the experimental group was significantly greater than in the control group (Fig. 1A).

Comparative histomorphometric study of ischemic lesions in skeletal muscle tissue

The excision surgery induced formation of ischemic foci in various portions of calf muscles. These foci, as observed on days 3 and 10 after transplantation (respectively, days 10 and 17 after surgery), contained multitudes of necrotized muscle fibers (identified by characteristic swelling and lack of nuclei at the periphery) and massive lymphohistiocytic infiltrations. On day 10 after transplantation the infiltrations still accompanied the atrophied and the individually found necrotized muscle fibers similarly in both groups. On day 30 after transplantation necrotization of individual

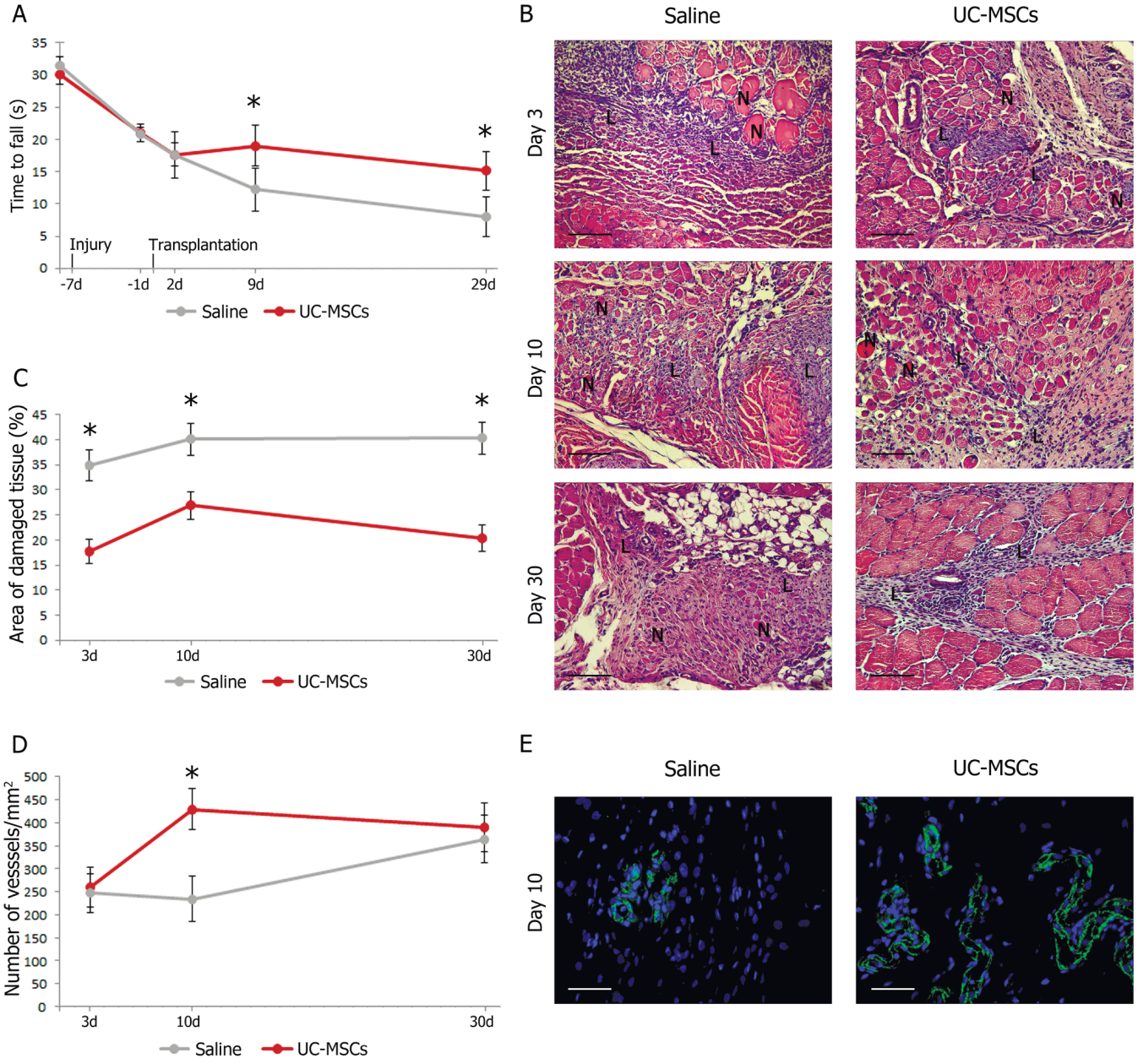

Fig. 1. Beneficial effects of UC-MSC transplantation applied to rat model of sustained limb ischemia. **A.** Rotarod test results expressed as mean±SD; *P<0.05. **B.** Representative images of morphological alterations in the ischemic muscles. H&E staining. N: necrotized muscle fibers; L: lymphohistiocytic infiltrations. **C.** Histomorphometric values expressed as mean±SD; *P<0.05. **D.** Blood vessel densities expressed as mean±SD; *P<0.05. **E.** Representative images of anti-CD31 immunostaining (green). Blue corresponds to cell nuclei counterstained with DAPI. Scale bars: B, 100 μm; E, 50 μm.

muscle fibers persisted and diffuse infiltrations were still observed in the control group, while in the experimental group the damaged muscle fibers were replaced by newly formed layers of fibrous tissue (Fig. 1B).

The area of ischemic damage was significantly smaller in the experimental group than in the control group throughout the observation (Fig. 1C).

Comparative histomorphometric assessment of revascularization

Total numbers of microcirculation vessels (arterioles, venules, and capillaries) per unit area did not differ significantly between the groups on day 3 after transplantation, but were significantly higher in the experimental group than in the control group on day 10 after transplantation (respectively, 429.4±44.6 per 1 mm^2 and 234.0±19.1 per 1 mm^2). Later on, this effect was obliterated, and no significant difference in microcirculation vessel densities was found between the groups on day 30 after transplantation (Fig. 1D,E).

Tracing localization of transplanted UC-MSCs

Clusters of PKH26-labeled cells, obviously corresponding to injection tracks, were clearly visualized within the lesions on day 3 after transplantation. Some of the PKH26-labeled cells were located in central portions of ischemic foci, and some of them were found at the borders, in the vicinity of preserved muscle fibers. On day 10 after transplantation clusters of PKH26-labeled cells were still observed in some portions of the foci; however, their distribution became more scattered by this time, and some labeled cells were observed in perimysia of the perifocal area. On day 30 after transplantation all PKH26-labeled cells were confined to

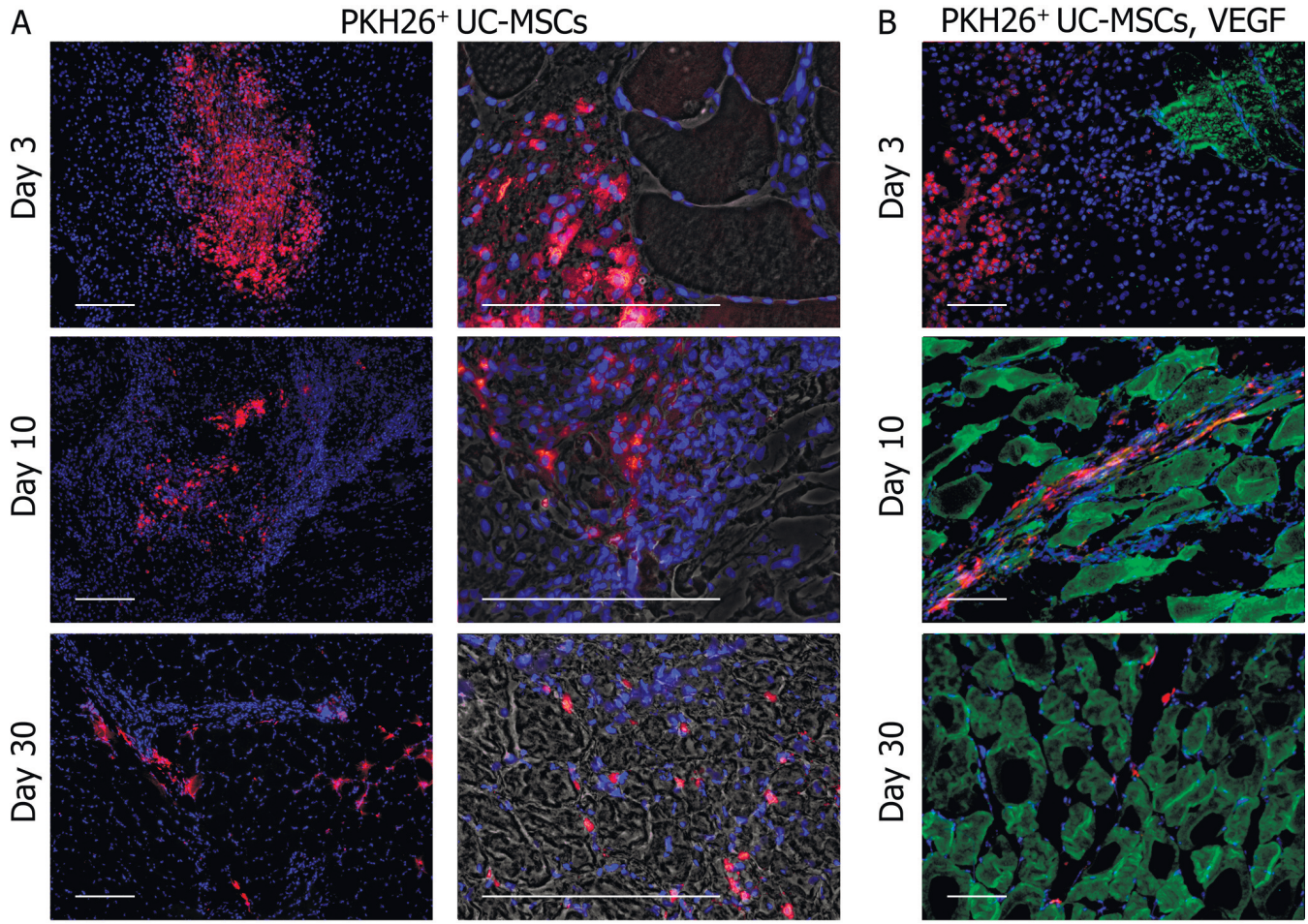

Fig. 2. Tracing of transplanted UC-MSCs in host tissues. **A.** Representative fluorescence and phase contrast microscopy images of PKH26-comprising cells (red) in the vicinity of injection site on days 3, 10, and 30 after transplantation. Cell nuclei counterstained with DAPI (blue). **B.** Representative images of PKH26-positive cells (red) migrating towards perimysium of VEGF-producing skeletal muscle fibers. Green corresponds to anti-VEGF immunostaining, blue corresponds to cell nuclei counterstained with DAPI. Scale bars: A, 200 μm; B, 100 μm.

layers of connective tissue and the perimysium (Fig. 2A).

Immunohistochemical staining showed that the preserved muscle fibers of the perifocal area produced VEGF, while the transplanted UC-MSCs did not (Fig. 2B).

Tracing elimination of transplanted UC-MSCs by host macrophages

Immunohistochemical staining of cryosections with anti-CD68 antibody revealed that some of the CD68+ cells also contained the PKH26 label, which was indicative of the capture of labeled membranous fragments by resident macrophages (Fig. 3A). The proportion of these double-positive cells was increasing in time; accordingly, the Mander's overlap coefficient for corresponding signals increased significantly from 0.70±0.03 on day 3 to 0.86±0.04 on day 30 after transplantation (Fig. 3B).

Tracing differentiation of transplanted UC-MSCs

We observed no signs of differentiation of PKH26-labeled cells into endothelial cells (Fig. 3C). Similarly, no PKH26-labeled smooth muscle cells were observed, although some of the transplanted cells retained the αSMA expression (Fig. 3D). In general, the PKH26-labeled cells were totally absent from the walls of capillaries and larger vessels throughout the observation.

Influence of transplanted UC-MSCs on macrophage infiltration and polarization at the site of injury

Cells expressing the macrophage-specific antigen CD68 were clearly visualized within ischemic foci, their shapes varying from round to fusiform (Fig. 4A). Relative numbers of these CD68+ cells were especially high in the control group, where they reached 56.22±5.46% on day 3 after transplantation (day 10 after surgery; significantly greater than in the experimental group on the same day, 45.30±2.38%). Macrophage infiltrations were gradually reduced in both groups, and no differences in relative numbers of CD68+ cells between the groups were observed on days 10 and 30 after transplantation (Fig. 4B).

Cells expressing CD206, the alternatively activated M2a and M2c macrophage-specific antigen (Gensel and Zhang, 2015), were also present in the foci, and these were always large cells of round shape (Fig. 4A).

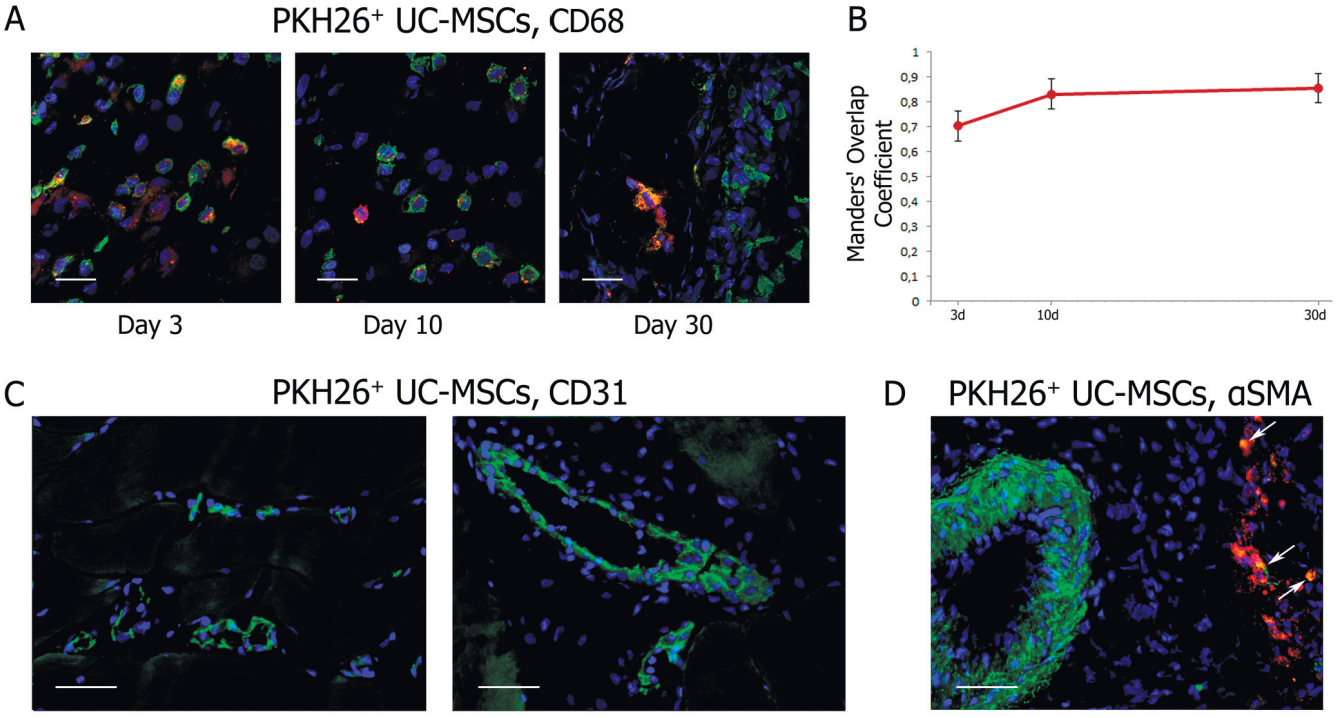

Fig. 3. Survival and stability of transplanted UC-MSCs in host tissues. **A.** Representative confocal microscopy image showing elimination of transplanted UC-MSCs by host macrophages within ischemic foci, as indicated by presence of cells double-positive for PKH26 and CD68 (red and green signals, respectively). **B.** Measured colocalization between the signals. **C.** Nonappearance of PKH26 label in endothelium of blood capillaries (left) and larger blood vessels (right); green corresponds to anti-CD31 immunostaining. Cell nuclei counterstained with DAPI (blue). **D.** Nonappearance of PKH26 label in smooth muscle elements of blood vessels; white arrows indicate cells that are double-positive for PKH26 and αSMA (red and green signals, respectively). Scale bars: 50 μm.

Relative numbers of CD206+ cells in the experimental group reached 42.05±2.77% on day 3 after transplantation (day 10 after surgery). A gradual reduction in their numbers followed a reciprocal trend: by day 10 after transplantation relative numbers of CD206+ cells in the experimental group diminished, still remaining significantly higher than in the control group (respectively, 33.33±3.06% and 26.34±3.5%), and by day 30 after transplantation relative numbers of CD206+ cells in both groups leveled (Fig. 4B).

Discussion

Excision of femoral and popliteal arteries in a rat prevents oxygenated blood from entering the limb, thereby causing profound necrotic changes within calf muscles, with severe and prolonged inflammatory response and subsequent scar formation. Characteristic response of muscle tissue to ischemic intervention of this type (Laurila et al., 2009; Rigamonti et al., 2013; Pellegrin et al., 2014) was successfully reproduced in this study, as confirmed by the histological analysis (Fig. 1B).

Functional condition of muscular system of animals that underwent the ischemic surgical intervention with subsequent transplantation of stromal/stem cells (either true, or sham) was evaluated at intervals by using the rotarod performance test. Animals of experimental group responded to the transplantation by temporary improvement in their locomotor function. This effect was not immediate, but gradually evolved over time; significant differences between the groups, recorded by day 9 after transplantation, persisted during the whole time length of the experiment (Fig. 1A). Histomorphometric analysis showed that relative area of the lesions in the experimental group was significantly smaller than in the control group at all time points during the observation (Fig. 1C). Descriptions of similar effects were found in literature for allogeneic transplantation of bone marrow-derived MSCs in mouse model of limb ischemia (Cunha et al., 2013).

Progression of neoangiogenesis within ischemic foci was assessed by histomorphometry using immunostaining of the endothelial marker CD31 (Fig. 1E). Calculated densities of microcirculation vessels within the lesions were significantly higher in the experimental group than in the control group on day 10 after transplantation (that is, on day 17 after surgery), but the difference smoothed out by day 30 after transplantation (Fig. 1D). Similar differences in blood vessel densities were recorded by Choi et al. for corresponding mouse model on day 21 after transplantation, and this similarity is remarkable given that the authors used another species of rodents and that the transplantation of UC-MSCs in their setting was undertaken at only 6 hours after ischemic intervention (Choi et al., 2013).

Altogether, the experiment provided an UC-MSC-mediated improvement in structural and functional

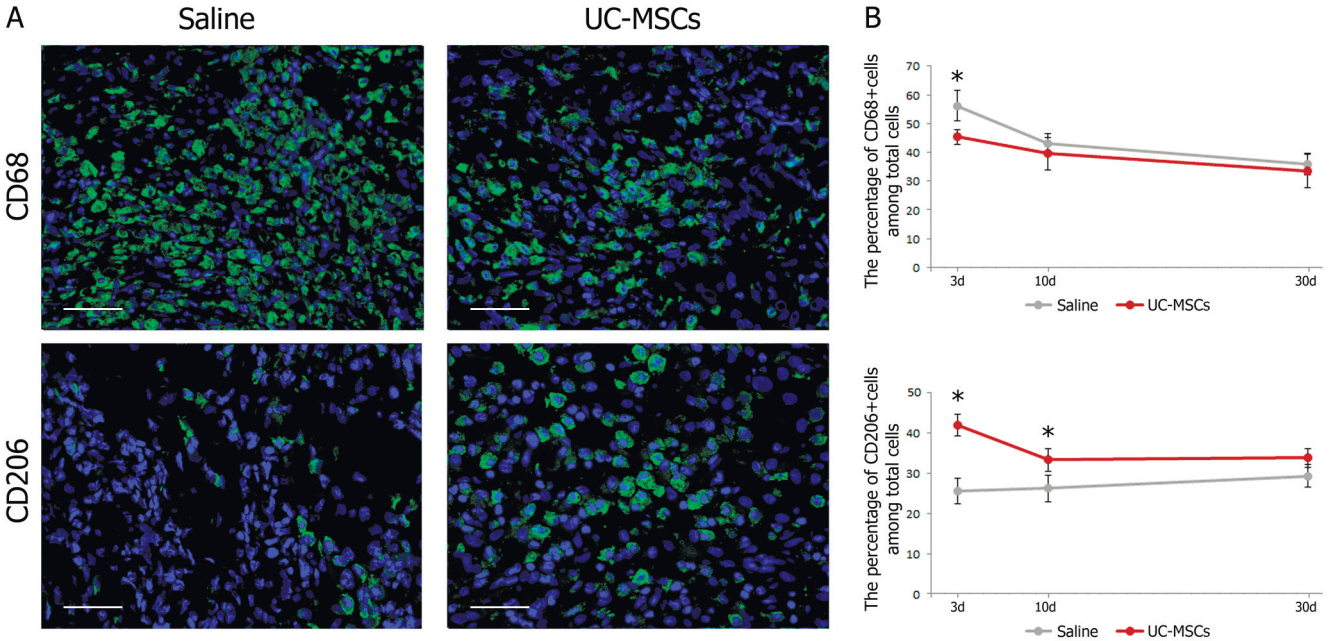

Fig. 4. Influence of transplanted UC-MSCs on macrophage infiltration and polarization at the site of injury. **A.** Representative images of CD68+ cells (upper) and CD206+ cells (lower) present in the ischemic skeletal muscle tissue on day 3 after transplantation. Green corresponds to immunostaining, blue corresponds to cell nuclei counterstained with DAPI. **B.** Relative counts of CD68+ and CD206+ cells expressed as mean±SD; *P<0.05. Scale bars: 50 μm.

condition of ischemic skeletal muscles, which was highly reproducible and therefore suitable for studying its mechanisms.

Shortly after being transplanted, the PKH26-labeled UC-MSCs started to abandon the clusters initially formed along injection tracks (still clearly observable on day 3 after transplantation) and distributed diffusely within the ischemic foci and in the perimysium of perifocal area, where undamaged muscle fibers were preserved (Fig. 2A). These fibers actively produced VEGF (Fig. 2B), which is known to attract MSCs *in vitro* (Rachakatla et al., 2007; Beckermann et al., 2008) and *in vivo* (Taghavi and George, 2013).

Although the PKH26 label was clearly observable on cryosections at all time points during the experiment, the affiliation of this label to a particular cell type should be discussed taking into account some current and previous findings. Notably, on cryosections stained with macrophage-specific anti-CD68 antibody some of the CD68+ also look as if they were PKH26-labeled, indicating capturing of the label by resident macrophages (Fig. 3A). This effect has been described in our recent study, according to which some of the PKH26-comprising cells are also identified as CD68+ cells shortly after transplantation, the proportion of such cells significantly increases from 48.1±3.2% on day 3 to 76.2±3.9% on day 30 after transplantation, as calculated for this particular model, and this is apparently a consequence of incorporation of transplanted labeled cells or their fragments by resident macrophages by means of phagocytosis (Arutyunyan et al., 2015).

Thus, only a part of the transplanted allogeneic UC-MSCs survived within the ischemic muscle tissue, and a considerable portion of these surviving cells were found alongside the VEGF-producing preserved muscle fibers (Fig. 2B). Within the intact muscle, VEGF is produced by satellite cells only (Germani et al., 2003), whereas hypoxic conditions induce synthesis of VEGF by muscle fibers in a HIF1-dependent manner (Wang et al., 2014). Thus, the transplanted cells were immediately exposed to action of VEGF, a major factor of endothelial cell differentiation. Despite that, the PKH26 label has not been found within the walls of capillaries or larger blood vessels, as revealed by anti-CD31 and anti-αSMA immunostaining (Fig 3C,D). Apparently, no evidence of UC-MSC differentiation into endothelial cells upon transplantation to ischemic skeletal muscles has ever been reported, although it was scrupulously searched for (Choi et al., 2013). Besides, the measured VEGF levels in ischemic tissues are approx. 10^3 lower than in culture media supplemented with up to 50 ng/ml of this factor, used to obtain the endothelial-like differentiation of MSCs *in vitro* (Jiang et al., 2014) and the general capacity of MSCs to differentiate into endothelial cells *in vivo* is often questioned (Bronckaers et al., 2014). It is important to note that at all time points during observation (that is, until day 30 after transplantation) some of the label-comprising cells remained αSMA-positive (Fig. 3D). Considering that αSMA is not expressed by macrophages (He and Marneros, 2013), this means that a portion of the transplanted UC-MSCs retained the characteristic αSMA-positive myofibroblast-like phenotype described elsewhere (Ohta, 2013) throughout the entire observation period.

The results suggest that potential cell replacement mechanisms can hardly be considered a leading mode in implementation of the proangiogenic activity of UC-MSCs *in vivo*. No differentiation of the transplanted cells into endothelial progeny has been observed, while a substantial portion of them was eventually eliminated by the host immune system.

Another, most recently suggested potential mechanism of therapeutic activity of MSCs is based on their ability to switch the classical M1 pathway of macrophage activation to the alternative M2 pathway (Dayan et al., 2011); in connection with this concept, a separate part of the current study dealt with possible effects of UC-MSC transplantation on macrophage infiltration and polarization at the site of injury.

Ischemic injuries to skeletal muscle tissue, induced in rats and mice by standardized surgical interventions, typically lead to development of vascular necrosis accompanied by pronounced inflammatory infiltration. It is initially dominated by neutrophils, which become eventually replaced by macrophages at about 3 days after ischemic intervention (Rigamonti et al., 2014). Later on, the influx of CD68+ cells gradually ceases (Laurila et al., 2009; Pellegrin et al., 2014). Very high relative counts of macrophages in the ischemic foci (e.g. 56.22±5.46% of all cells on day 10 after surgery; Fig. 4B) correspond to absolute counts of 1 to 2.5×10^3 macrophages per 1 mm^2 of section area, which is close to literary data (Laurila et al., 2009; Zordan et al., 2014).

It is known that blocking of macrophage infiltration considerably impairs regeneration of ischemic skeletal muscle tissue (Shireman et al., 2007; Contreras-Shannon et al., 2007). However, the roles of individual macrophage subpopulations in the aftermath of ischemia remain largely unspecified. Our results are consistent with the idea that ischemic foci become enriched in activated macrophages of M2 type (Pellegrin et al., 2014; Zordan et al., 2014). We show that an intramuscular injection of allogeneic UC-MSCs significantly increases the proportion of M2 macrophages, exhibiting proangiogenic and anti-inflammatory properties, for at least 10 days following the transplantation (Fig. 4B). Similar results have been recently reported by Kang et al. (the authors describe stimulation of M2 macrophage infiltration by UC-MSCs in a thrombosis induced limb ischemia mouse model (Kang et al., 2016)), and there is also clinical evidence of the immunomodulatory effects of UC-MSCs exerted by shifting local patterns of macrophage polarization (Gao et al., 2016).

The main putative mechanism of UC-MSC-mediated macrophage activation is paracrine; this idea is supported by evidence that M2 activation/polarization of macrophages can be promoted *in vivo* by UC-MSC-

conditioned culture medium (Shohara et al., 2012). Prostaglandin E2 (PGE2) is believed to be a major mediator of M2 pathway of macrophage activation (Prockop, 2013). Production of PGE2 by UC-MSCs *in vitro* is substantially upregulated by proinflammatory cytokines IL-1β and TNFα (Sabapathy et al., 2014). At 3 days after ischemic injury to skeletal muscle, local concentrations of these cytokines rise approx. 31-fold and 12-fold, respectively, and are maintained at these levels for up to 3 weeks (Fan et al., 2013). A transient increase in local concentrations of IL-1β and TNFα is probably a prerequisite for success of cell therapy, and this is consistent with reported evidence: administration of MSCs at 1 week after surgical induction of ischemia restores blood supply within the injured limb more effectively than transplantation at 24 hours after the induction (Moon et al., 2006), and the latest terms of therapeutically relevant administration of MSCs to the ischemic limb constitute 10 days for mice and 3 weeks for rats (Liew and O'Brien, 2012). As projected to the results of this study, these findings implicate that the high content of proinflammatory cytokines IL-1β and TNFα in ischemic muscle on day 7 after injury has stimulated secretion of PGE2 by the transplanted cells, and the massive release of PGE2 by the transplanted cells has subsequently triggered M2 activation of macrophages. Furthermore, PGE2 secreted by MSCs might also prevent activation of other cells of the immune system, including natural killer cells, granulocytes, dendritic cells and T1 helper cells, although systemic administration of PGE2 has a pro-inflammatory effect (Madrigal et al., 2014).

By stimulating the M2 pathway of macrophage activation, UC-MSCs largely determine local cytokine profiles, which in turn affect the character of inflammatory response, as well as angiogenic processes. In particular, M2 macrophages provide a local source of HGF during early stages of muscle tissue recovery (Sawano et al., 2014). They also produce a variety of pro-angiogenic factors including VEGF, FGFb, IGF-1, MCP-1, and PGF; notably, M2a macrophages stimulate angiogenesis via FGF-mediated pathway, whereas the effects of M2c macrophages are predominantly mediated by PGF (Wu et al., 2010; Jetten et al., 2014). Additionally, M2a macrophages secrete substantial amounts of PDGF-BB, whereas M2c macrophages secrete MMP9, thereby providing joint support to the sprouting of endothelial cells by accomplishing the extracellular matrix remodeling and pericyte recruitment (Spiller et al., 2014). It has been recently demonstrated for a model of myocardial infarction that a local joint delivery of FGF and HGF attracts M2 macrophages to the focus of ischemic damage and results in accelerated revascularization of the area, while inhibition of the macrophage infiltration impedes the angiogenesis. Analysing their results, the authors came up with a concept of "pro-angiogenic macrophages" (Barbay et al., 2015).

Thus, UC-MSCs transplanted into ischemic muscles act as a regulator of inflammation and enhance tissue repair by modulating local patterns of macrophage activation. This modulation appears to be one of the main mechanisms of their therapeutic action, and the possibility of its fine tuning is of great importance for basic research and clinical practice.

Conclusions

An intramuscular injection of allogeneic UC-MSCs facilitates recovery of surgically ischemic skeletal muscle tissue in rat model, as manifested by a decrease in the size of ischemic focus, as well as reduced macrophage infiltration and improved microcirculatory vessel formation at the site of damage. Living transplanted PKH26+cells can be traced for up to 30 days after transplantation; UC-MSCs eventually migrate out of the site of injection to become diffusely distributed within the focus and also in perimysium of the perifocal zone. However, immunostaining with antibodies to the macrophage-specific marker CD68+ shows that some of these cells are macrophages, which have captured the label by phagocytosis. The proportion of macrophages among the labeled cells is increased with time. The appearance and expansion of CD68+PKH26+ cells may be considered as a result of phagocytosis of transplanted labeled cells, or their fragments, by macrophages *in vivo*; this finding contradicts the concept of immune privilege conventionally ascribed to UC-MSCs.

At the same time, a certain portion of the transplanted UC-MSCs survives within the ischemized muscle for a long time and is exposed to endogenous VEGF, which is produced by the preserved muscle fibers. No clear experimental confirmation has been obtained, however, for *in vivo* differentiation of these cells into endothelial or smooth muscle cells of blood vessels. Immunohistochemical study has confirmed the suggestion that the therapeutic effect of the UC-MSC transplantation is achieved via temporary stimulation of the activation of pro-angiogenic and anti-inflammatory M2 macrophages in the area of damage.

Acknowledgments. This paper was financially supported by Ministry of Education and Science of the Russian Federation on the program to improve the competitiveness of Peoples' Friendship University (RUDN University) among the world's leading research and education centers in the 2016-2020. Part of this work including isolation, expansion, and characterization of UC-MSCs was supported by the Russian Science Foundation (Project No. 16-15-00281).

Conflicts of Interest. The authors declare that there is no conflict of interest regarding the publication of this article.

References

Arutyunyan I., Elchaninov A., Fatkhudinov T., Makarov A., Kananykhina E., Usman N., Bolshakova G., Glinkina V., Goldshtein D. and Sukhikh G. (2015). Elimination of allogeneic multipotent stromal cells

by host macrophages in different models of regeneration. Int. J. Clin. Exp. Pathol. 8, 4469-4480.

Arutyunyan I., Elchaninov A., Makarov A. and Fatkhudinov T. (2016a). Umbilical cord as prospective source for mesenchymal stem cell-based therapy. Stem Cells Int. 2016, 6901286.

Arutyunyan I., Fatkhudinov T., Kananykhina E., Usman N., Elchaninov A., Makarov A., Bolshakova G., Goldshtein D. and Sukhikh G. (2016b). Role of VEGF-A in angiogenesis promoted by umbilical cord-derived mesenchymal stromal/stem cells: *in vitro* study. Stem Cell Res. Ther. 7, 46.

Barbay V., Houssari M., Mekki M., Banquet S., Edwards-Lévy F., Henry J.P., Dumesnil A., Adriouch S., Thuillez C., Richard V. and Brakenhielm E. (2015). Role of M2-like macrophage recruitment during angiogenic growth factor therapy. Angiogenesis 18, 191-200.

Beckermann B.M., Kallifatidis G., Groth A., Frommhold D., Apel A., Mattern J., Salnikov A.V., Moldenhauer G., Wagner W., Diehlmann A., Saffrich R., Schubert M., Ho A.D., Giese N., Büchler M.W., Friess H., Büchler P. and Herr I. (2008). VEGF expression by mesenchymal stem cells contributes to angiogenesis in pancreatic carcinoma. Br. J. Cancer 99, 622-631.

Bronckaers A., Hilkens P., Martens W., Gervois P., Ratajczak J., Struys T. and Lambrichts I. (2014). Mesenchymal stem/stromal cells as a pharmacological and therapeutic approach to accelerate angiogenesis. Pharmacol. Ther. 143, 181-96.

Choi M., Lee H.S., Naidansaren P., Kim H.K., O E., Cha J.H., Ahn H.Y., Yang P.I., Shin J.C. and Joe Y.A. (2013). Proangiogenic features of Wharton's jelly-derived mesenchymal stromal/stem cells and their ability to form functional vessels. Int. J. Biochem. Cell Biol. 45, 560-570.

Contreras-Shannon V., Ochoa O., Reyes-Reyna S.M., Sun D., Michalek J.E., Kuziel W.A., McManus L.M. and Shireman P.K. (2007). Fat accumulation with altered inflammation and regeneration in skeletal muscle of CCR2-/- mice following ischemic injury. Am. J. Physiol. Cell Physiol. 92, 953-967.

Cunha F.F., Martins L., Martin P.K., Stilhano R.S. and Han S.W. (2013). A comparison of the reparative and angiogenic properties of mesenchymal stem cells derived from the bone marrow of BALB/c and C57/BL6 mice in a model of limb ischemia. Stem Cell Res. Ther. 4, 86.

Dayan V., Yannarelli G., Billia F., Filomeno P., Wang X.H., Davies J.E. and Keating A. (2011). Mesenchymal stromal cells mediate a switch to alternatively activated monocytes/macrophages after acute myocardial infarction. Basic Res. Cardiol. 106, 1299-1310.

Donders R., Vanheusden M., Bogie J.F., Ravanidis S., Thewissen K., Stinissen P., Gyselaers W., Hendriks J.J. and Hellings N. (2015). Human Wharton's jelly-derived stem cells display immunomodulatory properties and transiently improve rat experimental autoimmune encephalomyelitis. Cell Transplant. 24, 2077-2098.

Gao W.H., Yu J.Y., Li H.M., Guan Y., Li S.Z. and Huang P.P. (2016). The immunomodulatory effects of umbilical cord mesenchymal stem cell in critical limb ischemia patients. J. Stem Cell Res. Ther. 6, 349.

Gensel J.C. and Zhang B. (2015). Macrophage activation and its role in repair and pathology after spinal cord injury. Brain Res. 1619, 1-11.

Germani A., Di Carlo A., Mangoni A., Straino S., Giacinti C., Turrini P., Biglioli P. and Capogrossi M.C. (2003). Vascular endothelial growth factor modulates skeletal myoblast function. Am. J. Pathol. 163, 1417-1428.

Han K.H., Kim A.K., Kim M.H., Kim D.H., Go H.N. and Kim D.I. (2016). Enhancement of angiogenic effects by hypoxia-preconditioned human umbilical cord-derived mesenchymal stem cells in a mouse model of hindlimb ischemia. Cell Biol. Int. 40, 27-35.

He L. and Marneros A.G. (2013). Macrophages are essential for the early wound healing response and the formation of a fibrovascular scar. Am. J. Pathol. 182, 2407-2417.

Ishikane S., Ohnishi S., Yamahara K., Sada M., Harada K., Mishima K., Iwasaki K., Fujiwara M., Kitamura S., Nagaya N. and Ikeda T. (2008). Allogeneic injection of fetal membrane-derived mesenchymal stem cells induces therapeutic angiogenesis in a rat model of hind limb ischemia. Stem Cells 26, 2625-2633.

Iwase T., Nagaya N., Fujii T., Itoh T., Murakami S., Matsumoto T., Kangawa K. and Kitamura S. (2005). Comparison of angiogenic potency between mesenchymal stem cells and mononuclear cells in a rat model of hindlimb ischemia. Cardiovasc. Res. 66, 543-551.

Jetten N., Verbruggen S., Gijbels M.J., Post M.J., De Winther M.P. and Donners M.M. (2014). Anti-inflammatory M2, but not pro-inflammatory M1 macrophages promote angiogenesis *in vivo*. Angiogenesis 17, 109-118.

Jiang Q., Ding S., Wu J., Liu X. and Wu Z. (2014). Norepinephrine stimulates mobilization of endothelial progenitor cells after limb ischemia. PLoS One 9, e101774.

Kalaszczynska I. and Ferdyn K. (2015). Wharton's jelly derived mesenchymal stem cells: future of regenerative medicine? Recent findings and clinical significance. Biomed. Res. Int. 2015, 430847.

Kang W.C., Oh P.C., Lee K., Ahn T. and Byun K. (2016). Increasing injection frequency enhances the survival of injected bone marrow derived mesenchymal stem cells in a critical limb ischemia animal model. Korean J. Physiol. Pharmacol. 20, 657-667.

Kim Y., Kim H., Cho H., Bae Y., Suh K. and Jung J. (2007). Direct comparison of human mesenchymal stem cells derived from adipose tissues and bone marrow in mediating neovascularization in response to vascular ischemia. Cell Physiol. Biochem. 20, 867-876.

Laurila J.P., Laatikainen L.E., Castellone M.D. and Laukkanen M.O. (2009). SOD3 reduces inflammatory cell migration by regulating adhesion molecule and cytokine expression. PLoS One 4, e5786.

Liew A. and O'Brien T. (2012). Therapeutic potential for mesenchymal stem cell transplantation in critical limb ischemia. Stem Cell Res. Ther. 3, 28.

Lin Y., Lin L., Wang Q., Jin Y., Zhang Y., Cao Y. and Zheng C. (2015). Transplantation of human umbilical mesenchymal stem cells attenuates dextran sulfate sodium-induced colitis in mice. Clin. Exp. Pharmacol. Physiol. 42, 76-86.

Liu L., Mao Q., Chu S., Mounayar M., Abdi R., Fodor W., Padbury J.F. and De Paepe M.E. (2014). Intranasal versus intraperitoneal delivery of human umbilical cord tissue-derived cultured mesenchymal stromal cells in a murine model of neonatal lung injury. Am. J. Pathol. 184, 3344-3358.

Madrigal M., Rao K.S. and Riordan N.H. (2014). A review of therapeutic effects of mesenchymal stem cell secretions and induction of secretory modification by different culture methods. J. Transl. Med. 12, 260.

Moon M.H., Kim S.Y., Kim Y.J., Kim S.J., Lee J.B., Bae Y.C., Sung S.M. and Jung J.S. (2006). Human adipose tissue-derived mesenchymal stem cells improve postnatal neovascularization in a mouse model of hindlimb ischemia. Cell Physiol. Biochem. 17, 279-290.

Norgren L., Hiatt W.R., Harris K.A. and Lammer J. and TASC II Working Group (2007). TASC II section F on revascularization in PAD. J. Endovasc. Ther. 14, 743-744.

Ohta N. (2013). Umbilical cord matrix stem cells for cytotherapy of breast cancer. In: Stem cell therapeutics for cancer. Shah K. (ed). Wiley-Blackwell. pp 111-126.

Pellegrin M., Bouzourène K., Poitry-Yamate C., Mlynarik V., Feihl F., Aubert J.F., Gruetter R. and Mazzolai L. (2014). Experimental peripheral arterial disease: new insights into muscle glucose uptake, macrophage, and T-cell polarization during early and late stages. Physiol. Rep. 2, e00234.

Prockop D.J. (2013). Concise review: two negative feedback loops place mesenchymal stem/stromal cells at the center of early regulators of inflammation. Stem Cells 31, 2042-2046.

Rachakatla R.S., Marini F., Weiss M.L., Tamura M. and Troyer D. (2007). Development of human umbilical cord matrix stem cell-based gene therapy for experimental lung tumors. Cancer Gene Ther. 14, 828-835.

Rigamonti E., Touvier T., Clementi E., Manfredi A.A., Brunelli S. and Rovere-Querini P. (2013). Requirement of inducible nitric oxide synthase for skeletal muscle regeneration after acute damage. J. Immunol. 190, 1767-1777.

Sabapathy V., Sundaram B., Mankuzhy P. and Kumar S. (2014). Human Wharton's jelly mesenchymal stem cells plasticity augments scar-free skin wound healing with hair growth. PLoS One 9, e93726.

Santos J.M., Bárcia R.N., Simões S.I., Gaspar M.M., Calado S., Agua-Doce A., Almeida S.C., Almeida J., Filipe M., Teixeira M., Martins J.P., Graça L., Cruz M.E., Cruz P. and Cruz H. (2013). The role of human umbilical cord tissue-derived mesenchymal stromal cells (UCX®) in the treatment of inflammatory arthritis. J. Transl. Med. 11, 18.

Santos Nascimento D., Mosqueira D., Sousa L.M., Teixeira M., Filipe M., Resende T.P., Araújo A.F., Valente M., Almeida J., Martins J.P., Santos J.M., Bárcia R.N., Cruz P., Cruz H. and Pinto-do-Ó P. (2014). Human umbilical cord tissue-derived mesenchymal stromal cells attenuate remodeling after myocardial infarction by proangiogenic, antiapoptotic, and endogenous cell-activation mechanisms. Stem Cell Res. Ther. 5, 5.

Sawano S., Suzuki T., Do M.K., Ohtsubo H., Mizunoya W., Ikeuchi Y. and Tatsumi R. (2014). Supplementary immunocytochemistry of hepatocyte growth factor production in activated macrophages early in muscle regeneration. Anim. Sci. J. 85, 994-1000.

Shireman P.K., Contreras-Shannon V., Ochoa O., Karia B.P., Michalek J.E. and McManus L.M. (2007). MCP-1 deficiency causes altered inflammation with impaired skeletal muscle regeneration. J. Leukoc. Biol. 81, 775-785.

Shohara R., Yamamoto A., Takikawa S., Iwase A., Hibi H., Kikkawa F. and Ueda M. (2012). Mesenchymal stromal cells of human umbilical cord Wharton's jelly accelerate wound healing by paracrine mechanisms. Cytotherapy 14, 1171-1181.

Spiller K.L., Anfang R.R., Spiller K.J., Ng J., Nakazawa K.R., Daulton J.W. and Vunjak-Novakovic G. (2014). The role of macrophage phenotype in vascularization of tissue engineering scaffolds. Biomaterials 35, 4477-4488.

Taghavi S. and George J.C. (2013). Homing of stem cells to ischemic myocardium. Am. J. Transl. Res. 5, 404-411.

Wang T., Zhou Y.T., Chen X.N. and Zhu A.X. (2014). Putative role of ischemic postconditioning in a rat model of limb ischemia and reperfusion: involvement of hypoxia-inducible factor-1α expression. Braz. J. Med. Biol. Res. 47, 738-745.

Wu W.K., Llewellyn O.P., Bates D.O., Nicholson L.B. and Dick A.D. (2010). IL-10 regulation of macrophage VEGF production is dependent on macrophage polarisation and hypoxia. Immunobiology 215, 796-803.

Zhang H.C., Liu X.B., Huang S., Bi X.Y., Wang H.X., Xie L.X., Wang Y.Q., Cao X.F., Lv J., Xiao F.J., Yang Y. and Guo Z.K. (2012). Microvesicles derived from human umbilical cord mesenchymal stem cells stimulated by hypoxia promote angiogenesis both *in vitro* and *in vivo*. Stem Cells Dev. 21, 3289-3297.

Zordan P., Rigamonti E., Freudenberg K., Conti V., Azzoni E., Rovere-Querini P. and Brunelli S. (2014). Macrophages commit postnatal endothelium-derived progenitors to angiogenesis and restrict endothelial to mesenchymal transition during muscle regeneration. Cell Death Dis. 5, e1031.

Accepted November 6, 2018